Catalyst-Assisted Formation of Nanocantilever Arrays on ZnS Nanoribbons by Post-Annealing Treatment

Yanqing Li, Kai Zou, Yue Yue Shan, Juan Antonio Zapien, and Shuit-Tong Lee*

Center of Super-Diamond and Advanced Films (COSDAF) and Department of Physics and Materials Science, City University of Hong Kong, Hong Kong SAR (P.R. China)

Received: September 6, 2005; In Final Form: December 15, 2005

Nanocantilever arrays were formed on the edges of the ±(0001) planes of pre-synthesized ZnS nanoribbons via catalyst-assisted post-annealing treatment on Si substrate at 600 °C. Similar nanostructures could also be generated when ZnS nanoribbons were annealed by mixing with Si or SiO powder. The formation of nanocantilever arrays is associated with orientation-dependent chemical etching of the ±(0001) polar surfaces of ZnS nanoribbons. The ability of increasing structural complexity beyond the one-step "thermal evaporation and condensation" synthesis provides a new dimension to the rational design of building blocks for nanodevices.

I. Introduction

Wurtzite-structured ZnS is an important II−VI compound semiconductor for a number of applications in ultraviolet light-emitting diodes, thin film electroluminescence, IR window, and other optoelectronic devices. Recently, nanoscale structures of ZnS, particularly in quasi one-dimensional nanostructures, have been the focus of intensive research as building blocks for nanoelectronic and nanophotonic systems.[1] Nanostructured materials with different morphologies such as nanowires, nanorods, nanoribbons, and nanocombs have been synthesized with highly crystalline quality and exhibit special electronic and optical properties.[2−8] For example, the synthesis of comb-like nanostructures comprising periodic nanocantilever arrays with identical diameters was reported and proposed to be associated with supersaturation or surface polarization.[7−10] The utilization of nanoscale materials inevitably requires full control of their structures for the "bottom-up" assemblies of nanodevices. Commonly, morphology-controlled growth of ZnS nanostructures was demonstrated via vapor transport and condensation during one-step synthesis. The capability of increasing structural complexity in a controlled manner is presently limited in the one-step growth, which would have much difficulty in achieving the rational design required for the building blocks in nanoscale fabrication.

Secondary growth or modification of preformed nanostructures can provide conceptually a new way for enabling the controlled synthesis of well-defined hierarchical nanoarchitectures. For example, branched nanowire structures have been synthesized via a multistep nanocluster-catalyzed vapor−liquid−solid (VLS) growth.[11,12] On the other hand, selective-area chemical etching to remove undesirable regions of materials is a technique used extensively in semiconductor processing to fabricate assemblies of sophisticated architecture for electronic and photonic devices. Through chemically reactive interaction, some special areas are preferentially dissolved. Often a specific crystal plane of single-crystal material is dissolved much faster than other planes, resulting in orientation-dependent etching. Such selective etching may thus offer an attractive capability for nanostructuring, but has not been sufficiently explored in nanoscale fabrication.

In this work, we report a catalyst-assisted formation of comb-like nanocantilever arrays grown perpendicularly from both sides of pre-synthesized ZnS nanoribbons along ±[0001] directions by simple post-annealing treatment. The formation of nanocantilever arrays is considered to be associated with the preferential chemical etching property of the ±(0001) surfaces of ZnS nanoribbons due to surface polarity.

II. Experimental Details

ZnS nanoribbons were synthesized in a horizontal quartz tube furnace by thermal evaporation of ZnS powder onto a Si substrate coated with Au catalyst. The synthetic reaction was carried out by heating the ZnS powder at 1050 °C for 2 h using high-purity Ar:5% H_2 (20 sccm) as carrier gas. After the reaction was finished and the furnace cooled to room temperature, a white wool-like product covering the substrate was obtained. For the post-annealing treatment, the ZnS nanoribbons were dispersed on Si substrates and then annealed at 600 °C for 30 min in an Ar atmosphere with a constant flow of 30 sccm. Additionally, annealing treatments were carried out by embedding the ZnS nanoribbons into high-purity Si or SiO powder. The products were systematically characterized using scanning electron microscopy (SEM; Philips XL 30 FEG), X-ray diffraction (XRD; Siemens D-500 with Cu Kα radiation and a normal 2θ scan), transmission electron microscopy (TEM; Philips CM20 at 200 kV), and high-resolution transmission electron microscopy (HRTEM; CM200 FEG, at 200 kV).

III. Results and Discussion

The SEM image in Figure 1a shows the as-synthesized product consists of a large quantity of nanoribbons with uniform geometry. From XRD, the structure of the nanoribbons was identified to be the hexagonal wurtzite-2H structure of ZnS with lattice constants of $a = 0.3825$ nm and $c = 0.6270$ nm, in good agreement with the Joint Committee on Powder Diffraction Standards (JCPDS) 36-1450 database. The nucleation and growth of ZnS nanoribbons were found to proceed via the metal-catalyzed VLS growth mechanism.[13] The presence of Au

* Corresponding author: E-mail: apannale@cityu.edu.hk, Fax: (852) 2784 4696.

10.1021/jp055026x CCC: $33.50 © 2006 American Chemical Society
Published on Web 03/16/2006

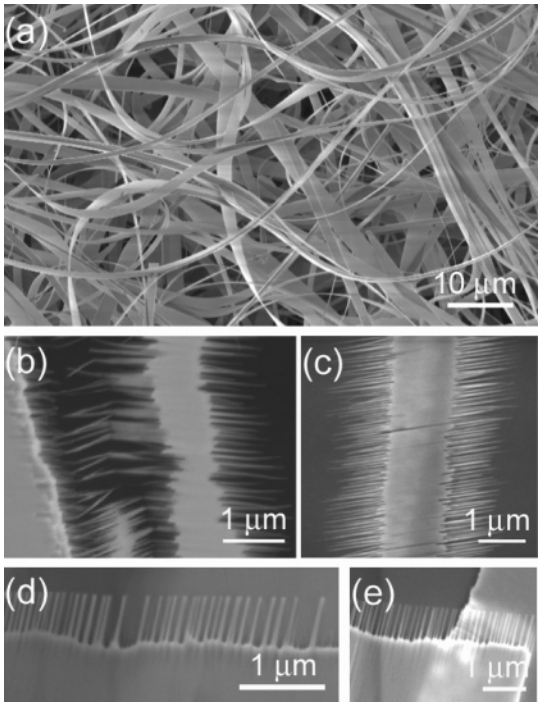

Figure 1. (a) SEM image of as-synthesized ZnS nanoribbons. (b−e) SEM images of representative nanocantilever arrays formed on the edge of ZnS nanoribbons dispersed on Si substrate by annealing at 600 °C for 30 min.

particles on the Si substrate is crucial to the formation of ZnS nanoribbons during the early stage of growth.[14] The uniform and flat morphology is driven by anisotropic growth kinetics along different crystallographic directions under a certain growth condition. Figures 1b−1e show the representative SEM images of the ZnS nanoribbons dispersed on the Si substrate after annealing treatment at 600 °C for 30 min. It can be seen that comb-like nanocantilever arrays were formed perpendicularly to both sides of the initial ZnS nanoribbons, and were perpendicular to their backbone. The results show that our approach can yield comb-like nanostructures similar to those obtained previously using one-step growth process.[7,8,10,15]

Detailed structural characterization of nanocantilever arrays on ZnS nanoribbons was carried out using TEM and HRTEM. Figures 2a and 2b show the typical TEM bright field images of ZnS nanocantilever arrays formed on both sides of nanoribbons. The nanocantilevers have diameters in the range of 3−15 nm and lengths up to 150 nm. The corresponding selected area electron diffraction (SAED) in the inset of Figure 2b indicates that the wurtzite-structured ZnS nanoribbons grow along [01$\bar{1}$0] direction. Together with the structure properties of the ribbon revealed by HRTEM, the top/bottom and side surfaces can be estimated to be ±(2$\bar{1}\bar{1}$0) and ±(0001) planes, respectively.[1,8,16]

HRTEM was applied to image the tip of the nanocantilever and the interspace between two adjacent nanocantilevers, respectively. The HRTEM image of Figure 2c illustrates the tip of a typical nanocantilever, showing it is single crystalline with a wurtzite structure. Figure 2d represents the HRTEM image recorded from the interspace region between two adjacent nanocantilevers. The measured interplanar spacing of 0.626 nm in Figures 2c and 2d corresponds to the distance between two {0001} lattice planes, indicating that the nanocantilevers, though of different diameters, are all parallel with the same direction of [0001]. No dislocations or defects induced by the annealing treatment are observed. Although no catalyst particles are present on the tip of the nanocantilever, some small nanoclusters are

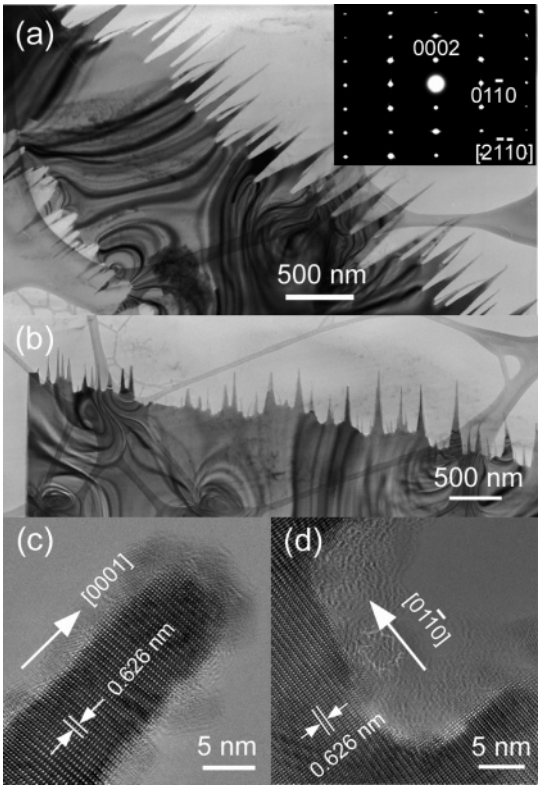

Figure 2. TEM images of ZnS nanocantilever structures formed on ZnS nanoribbons. (a, b) TEM images of comb-like ZnS nanostructures. The inset in (a) is the corresponding SAED pattern recorded on the entire structure along the [2$\bar{1}\bar{1}$0] zone axis. (c) HRTEM image of the tip region of a nanocantilever. (d) HRTEM image of the interspace region between two nanocantilevers.

observed to adhere to the surface of the nanocantilever, which may be associated with the formation of the nanocantilever structure. On the other hand, the junction between nanocantilever and the backbone of the nanoribbons exhibits single-crystal structure, which is in contrast to the formation of CdSe nanosaw structures accompanied with zinc blende−wurtzite phase transformation.[16]

Upon annealing treatment on Si substrate, ZnS nanocantilever arrays were formed on the ±(0001) planes of wurtzite-structured ZnS nanoribbons of [01$\bar{1}$0] orientation. This suggests that ±(0001) planes have preferential reactivity over the other planes. Similar comb-like nanostructures were commonly obtained at temperatures ranging from 500 to 900 °C,[7−9] and their growth mechanism was attributed to a spontaneous and self-catalyzed vapor−solid process.[7−9] However, in the present case, annealing treatment of pre-synthesized ZnS nanoribbons at 600 °C could not induce any change in morphology when the nanoribbons were not in contact with the Si substrate. This excludes the possibility of self-organization contributing to the formation of nanocantilever arrays on both sides of the initial nanoribbons. Instead, it suggests that the Si substrate is indispensable and serves as the catalyst in the nanostructure formation.

In view of the likely presence of residual oxygen due to leakage, we investigated the effect of oxygen environment on the morphology transformation during annealing treatment. The pre-synthesized ZnS nanoribbons were annealed in a pure O_2 atmosphere with a pressure of 6×10^{-2} Torr at 600 °C for 30 min. An SEM image of the obtained product (shown in Figure 3a) exhibits numerous interstices and spots but a lack of formation of nanocantilever structures on the edges of ZnS nanoribbons. TEM images of the resulting ZnS nanoribbons

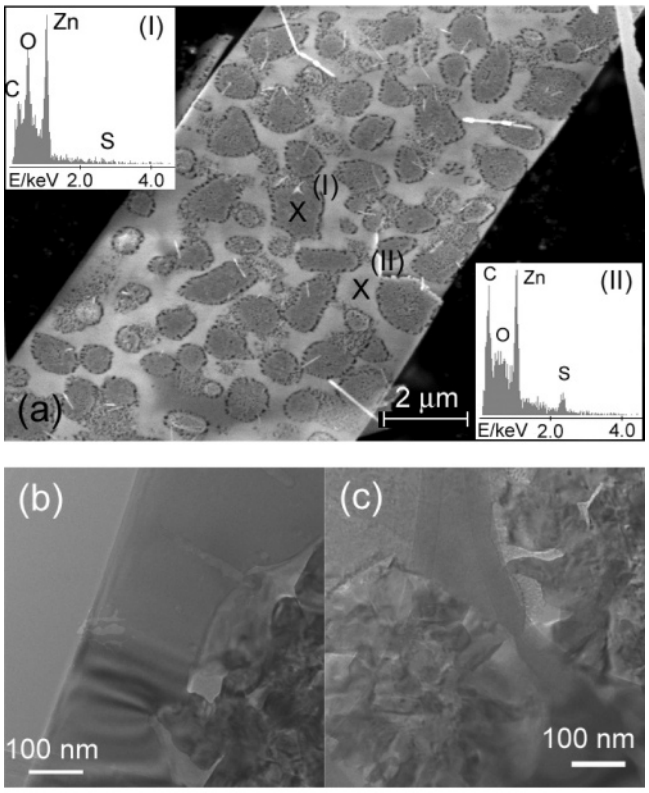

Figure 3. (a) SEM image of ZnS nanoribbons annealed in O_2 ambient at 600 °C. The insets are the EDX spectra of two selected regions as indicated. (b) and (c) TEM images of annealed ZnS nanoribbons showing numerous nanograins. (d) XRD pattern of wurtzite-structured ZnS nanoribbons with hexagonal wurtzite ZnO features.

shown in Figures 3b and 3c further confirm the formation of nanograins in the ZnS nanoribbons. Energy-dispersive X-ray spectroscopy (EDX) was performed in the selected regions as marked in Figure 3a. The stoichiometry in the black patches (position I) reveals the almost complete substitution of S with O. Figure 3d shows the XRD spectrum of the corresponding product. In addition to the features of wurtzite-structured ZnS, two new peaks appeared after annealing treatment, which can be assigned to hexagonal wurtzite ZnO with $a = 0.3249$ nm and $c = 0.5206$ nm (JCPDS 36-1451). The results thus show the formation of ZnO nanocrystals from the oxidation of ZnS nanoribbons, which is in good agreement with the oxygen beam treatment of ZnS nanowires.[17] The oxidation results also support that the Si substrate plays a determining role in the formation of nanocantilever arrays from the original ZnS nanoribbons.

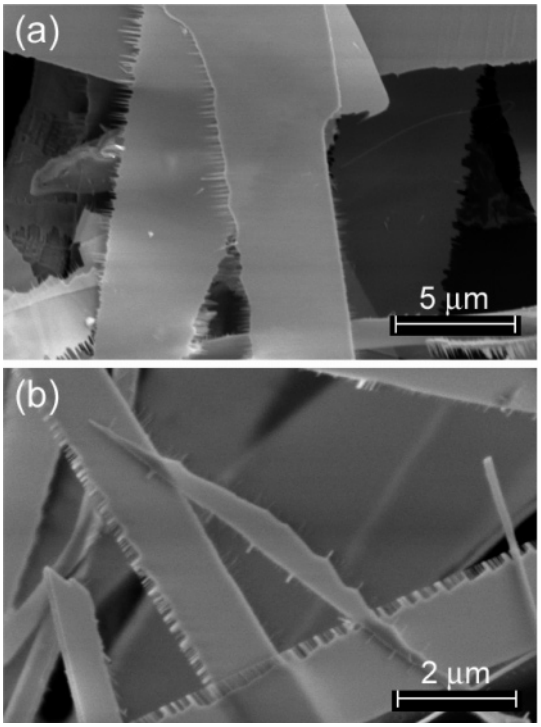

Figure 4. SEM images of ZnS nanoribbons annealed at 600 °C with a mixture of (a) Si powder and (b) SiO powder, respectively.

Further studies were carried out by annealing the ZnS nanoribbons embedded in SiO or Si powder under the same conditions. The residual powder was removed and washed off from the nanoribbons before any measurements. Surprisingly, nanocantilever arrays of similar morphology were formed on both sides of ZnS nanoribbons as shown in Figure 4. XRD spectra of 600 °C-annealed ZnS nanoribbons embedded in Si and SiO powder (not shown here) are shown to be almost identical to that of as-synthesized ZnS nanoribbons, indicating no phase changes due to annealing.

Although the detailed formation process of nanocantilever arrays on ZnS nanoribbons by post-annealing is not completely clear at this stage, we propose that it might be associated with a localized chemical etching process with the assistance of the catalyst. As wurtzite-structured ZnS is composed of alternately stacked planes along the *c* axial direction, terminated with either positively charged Zn^{2+} or negatively charged S^{2-} ions, the ZnS single crystal can therefore adopt two polar surfaces: the (0001)-Zn- and $(000\bar{1})$-S-terminated polar surfaces. On the other hand, the nonpolar surfaces such as $(2\bar{1}\bar{1}0)$ are formed by breaking the same number of Zn and S bonds. Consequently, the polar surfaces tend to possess distinctive surface properties, such as a higher chemical reactivity, compared with the nonpolar surfaces. Analogous to the ZnO surface as revealed by scanning tunneling microscopy,[18] we suppose that ZnS (0001)-Zn-terminated polar surface similarly comprises terraces and nanosized islands as well as many pits with S-terminated step edges, whereas $(000\bar{1})$-S-terminated surface is covered by hexagonal terraces. In general, the steps are relatively unstable in comparison to the terraces, so that the step-edge atoms could possibly offer the preferential sites for the redox reactions.

During the formation of nanocantilever arrays from ZnS nanoribbons, Si is shown to play a determining role in the nucleation of nanoclusters on the polar surface and subsequent redox reaction process. In the absence of Si substrate, Si powder, or SiO powder, no nanocantilever structures can be generated from the pre-synthesized ZnS nanoribbons. With the assistance

of catalyst, Si−Zn−S alloy might nucleate on the preferential sites of the (0001)-Zn− or (000$\bar{1}$)-S-terminated polar surfaces to form nanoclusters, thus the decomposition reaction and desorption process may more easily take place on ±(0001) surfaces. Subsequently, the built-in normal dipole moment due to the polar ZnS ±(0001) surface confines the decomposition direction normal to the surface, and the interaction of nanoclusters is preferentially enhanced at the concave corners between two branches rather than along the direction parallel to the surface. As a result, an inward-driven etching reaction occurs, leading to the V-shaped or straight-walled grooves and thereby the formation of comb-like nanostructures from the pre-synthesized ZnS nanoribbons.

The nanocantilever arrays formed on the edge of ZnS nanoribbons may find potential applications for nanodevices. For example, they may be used as diffraction gratings in miniaturized integrated optics,[10] Fabry−Perot optical cavities, or ultraviolet arrays.[7] In addition, such structures may be exploited in applications such as one-dimensional photonic crystals and nanometer electromechanical systems.

IV. Conclusions

We demonstrated the formation of self-assembled comb-like nanocantilever arrays grown perpendicularly to both sides of pre-synthesized ZnS nanoribbons via a simple catalyst-assisted post-annealing treatment. The formation of nanocantilever arrays is associated with the orientation-dependent chemical etching property on the ±(0001) polar surfaces of ZnS nanoribbons. Via optimizing the annealing condition, the concept of catalyst-assisted postannealing treatment presented here could be applied to generate highly defined hierarchical nanostructures based on pre-synthesized nanomaterials.

Acknowledgment. This work was supported by the Research Grants Council of Hong Kong (Project No. CityU 101504) and the Croucher Foundation, Hong Kong SAR, China.

References and Notes

(1) Jiang, Y.; Meng, X. M.; Liu, J.; Xie, Z. Y.; Lee, C. S.; Lee, S. T. *Adv. Mater*. **2003**, *15*, 323.
(2) Pan, Z. W.; Dai, Z. R.; Wang, Z. L. *Science* **2001**, *291*, 1947.
(3) Huang, M. H.; Mao, S.; Feick, H.; Yan, H.; Wu, Y.; Kind, H.; Webber, E.; Russo, R.; Yang, P. *Science* **2001**, *292*, 1897.
(4) Cui, Y.; Lieber, C. M. *Science* **2001**, *291*, 851.
(5) Zapien, J. A.; Jiang, Y.; Meng, X. M.; Chen, W.; Au, F. C. K.; Lifshitz, Y.; Lee, S. T. *Appl. Phys. Lett.* **2004**, *84*, 1189.
(6) Agarwal, R.; Barrelet, C. J.; Lieber, C. M. *Nano Lett*. **2005**, *5*, 917.
(7) Yan, H.; He, R.; Johnson, J.; Law, M.; Saykally, R. J.; Yang, P. *J. Am. Chem. Soc*. **2003**, *125*, 4728.
(8) Wang, Z. L.; Kong, X. Y.; Zuo, J. M. *Phys. Rev. Lett*. **2003**, *91*, 185502.
(9) Park, J. H.; Choi, H. J.; Choi, Y. J.; Sohn, S. H.; Park, J. G. *J. Mater. Chem*. **2004**, *14*, 35.
(10) Pan, Z. W.; Mahurin, S. M.; Dai, S.; Lowndes, D. H. *Nano Lett*. **2005**, *5*, 723.
(11) Dick, K. A.; Deppert, K.; Larsson, M.; Mårtensson, T.; Seifert, W.; Wallenberg, L. R.; Samuelson, L. *Nature Mater*. **2004**, *3*, 380.
(12) Wang, D.; Qian, F.; Yang, C.; Zhong, Z.; Lieber, C. M. *Nano Lett*. **2004**, *4*, 871.
(13) Wagner, R. S.; Ellis, W. C. *Appl. Phys. Lett*. **1964**, *4*, 89.
(14) Liu, Y. K.; Zapien, J. A.; Geng, C. Y.; Shan, Y. Y.; Lee, C. S.; Lifshitz, Y.; Lee, S. T. *Appl. Phys. Lett.* **2004**, *85*, 3241.
(15) Moore, D.; Ronning, C.; Ma, C.; Wang, Z. L. *Chem. Phys. Lett*. **2004**, *385*, 8.
(16) Ding, Y.; Ma, C.; Wang, Z. L. *Adv. Mater*. **2004**, *16*, 1740.
(17) Lin, M.; Zhang, J.; Boothroyd, C.; Foo, Y. L.; Yeadon, M.; Loh, K. P. *J. Phys. Chem. B* **2004**, *108*, 9631.
(18) Dulub, O.; Boatner, L. A.; Diebold, U. *Surf. Sci.* **2002**, *519*, 201.